ESAIM: PROCEEDINGS, August 2010, Vol. 30, p. 90-103
D. Bresch, V. Calvez, E. Grenier, P. Vigneaux & J.-F. Gerbeau, Editors

DIFFUSION MODELS OF MULTICOMPONENT MIXTURES IN THE LUNG *

L. Boudin[1, 2], D. Götz[3] and B. Grec[4, 5]

Abstract. In this work, we are interested in two different diffusion models for multicomponent mixtures. We numerically recover experimental results underlining the inadequacy of the usual Fick diffusion model, and the importance of using the Maxwell-Stefan model in various situations. This model nonlinearly couples the mole fractions and the fluxes of each component of the mixture. We then consider a subregion of the lower part of the lung, in which we compare the two different models. We first recover the fact that the Fick model is enough to model usual air breathing. In the case of chronic obstructive bronchopneumopathies, a mixture of helium and oxygen is often used to improve a patient's situation. The Maxwell-Stefan model is then necessary to recover the experimental behaviour, and to observe the benefit for the patient, namely an oxygen peak.

Introduction

The bronchial tree, which has a dyadic structure, can be schematically divided into two parts [19]. In the upper part of the airways (generations 0 to 14), the main phenomenon putting the air in motion is the convection, and the air can be described by the Navier-Stokes or the Stokes equations. In the lower part of the airways (generations 15 to 23), the gas behaviour is mainly diffusive, since the global velocity of the air is almost zero. We here consider this second distal part of the respiratory system, where the gaseous exchanges between the air and the blood take place.

For the sake of simplicity, we neglect the convection in the distal part of the bronchial tree, and only focus on the diffusive effects. Diffusion can be defined in a general way as the physical process that brings matter from one region of a system to another using random motions at a molecular level, see [5], for instance. The macroscopic diffusion model which is most commonly used is the Fick model (see, among many references, [7] in the framework of the lung), where the flux of a given species is directly proportional to its concentration gradient. At this level, the relevant unknowns appear to be the concentrations of each species (or any other proportional quantities).

There are several modelling issues in the diffusion phenomenon in the lung, which can be investigated: the diffusion model itself, which we tackle here, but also the geometry of interest, which cannot be determined by

* *This work was partially funded by the ANR-08-JCJC-013-01 project headed by C. Grandmont.*

[1] UPMC Paris 06, UMR 7598 LJLL, Paris, F-75005, France;
e-mail: laurent.boudin@upmc.fr

[2] INRIA Paris-Rocquencourt, REO Project team, BP 105, F-78153 Le Chesnay Cedex, France;

[3] TU Darmstadt, Fachbereich Mathematik, IRTG 1529, Schloßgartenstr. 7, D-64289 Darmstadt, Germany;
e-mail: goetz@mathematik.tu-darmstadt.de

[4] MAP5, CNRS UMR 8145, Université Paris Descartes, F-75006 Paris, France;
e-mail: berenice.grec@parisdescartes.fr

[5] Institut Camille Jordan, CNRS UMR 5208, Université Claude Bernard Lyon 1, F-69622 Villeurbanne, France

Article published online by EDP Sciences and available at http://www.esaim-proc.org or http://dx.doi.org/10.1051/proc/2010008

biological imaging, and has a great importance for the space and time scales, or the mechanism of gas exchange between the alveoli and the blood vessels through the alveolar membrane.

As far as the geometry is concerned, Kitaoka *et al.* [13] proposed a three-dimensional model of the human pulmonary acinus as a gas exchange unit built with a labyrinthine algorithm generating branching ducts, that completely fill a given space. Alveoli are attached to the inner walls of the space on study. They obtain physically relevant values for the total alveolar surface and the numbers of alveolar ducts, alveolar sacs, and alveoli. Mauroy also used the Kitaoka model of acinus in his PhD thesis [15].

Sapoval *et al.* [16] found out that efficient acini should be space-filling surfaces and should remain quite small. The efficiency depends on both the acini design and the values of physical factors like diffusivities of the gaseous components of the air in the airways and permeability of the membrane between the blood vessels and the alveoli.

In this work, we aim to check the relevance of two different diffusion models. The first one is the Fick model, which we already briefly presented. The main ideas of the second one were developed following independent pioneering works of Maxwell and Stefan, and we shall then refer to the Maxwell-Stefan model, as in [14]. This model takes into account the friction effects between different species.

We here show the shortcomings of the Fick model in some specific, but still realistic, situations in the lung. We provide numerical comparisons between Fick and Maxwell-Stefan's laws for the diffusion processes of various mixtures in the lower airways. In the case when the respiratory system is healthy, we recover the facts that both Fick and Maxwell-Stefan models are relevant, and that they provide results which are very close to each other. On the other hand, when one deals with patients who suffer from a severe airway obstruction, in the cases of chronic obstructive bronchopneumopathies (COBP), the ventilation has to happen faster. Thiriet *et al.* [18] led *in vivo* experiments and used a binary mixture of helium (79 %) and oxygen (21 %), which is usually called heliox (or oxhel), to speed up the oxygen transport towards the lower airways, so that the diffusion and the gaseous exchanges can more rapidly happen. We here point out, as suggested in [18], that when heliox is involved, the Fick law does not apply anymore. In [2], Chang obtains the same kind of result using some considerations on the model.

In our first section, we present the two diffusion processes of a multicomponent mixture, using the definition of the fluxes by Fick's and Maxwell-Stefan's laws. Then, in Section 2, we recall and numerically repeat the Duncan and Toor experiment that brought to light in the first place the interest of this more intricate model than Fick's. Eventually, we go back to the framework of the lung in Section 3 to compare the Fick and Maxwell-Stefan laws for the air in a two-dimensional branch, and point out some cases when the Fick law does not hold anymore.

1. Maxwell-Stefan vs. Fick's laws

Consider a gaseous mixture with M components, and assume they constitute an ideal gas mixture. The concentration c_i of species i, $1 \leq i \leq M$, depends on time $t \geq 0$ and space location $X \in \mathbb{R}^N$, $1 \leq N \leq 3$. If we denote $c_{\text{tot}} = \sum c_j$ the total concentration, the mole fraction x_i of species i is defined by $x_i = c_i/c_{\text{tot}}$. It satisfies the following mass conservation equation:

$$\partial_t x_i + \nabla_X \cdot \boldsymbol{N_i} = 0, \tag{1}$$

where $\boldsymbol{N_i} \in \mathbb{R}^N$ is the molar flux of species i. The expression of $\boldsymbol{N_i}$ with respect to the mole fractions $(x_j)_{1\leq j\leq M}$ depends on the diffusion model one chooses. Both cases are detailed in Subsection 1.2. We first present a brief physical derivation of Maxwell-Stefan's law in a one-dimensional setting.

1.1. Derivation of the Maxwell-Stefan law in one dimension

For the sake of simplicity, we momentarily assume $N = 1$ and consider a one-dimensional diffusion following the axis $X := X_1$. The force acting on species i in a control volume is given by $-\,\mathrm{d}p_i/\,\mathrm{d}X$, where p_i is the partial pressure of species i in the mixture.

Taking into account the ideal gas law $p_i = RTc_i$, where R is the ideal gas constant and T the absolute temperature, yields $(RT/c_i)(-\,\mathrm{d}c_i/\,\mathrm{d}X)$ for the force per mole of species i. At the equilibrium, this force is balanced by the drag (or friction) forces exerted by the other species in the mixture. It is standard to assume that the drag force is proportional to the relative velocity as well as to the mole fraction of the other components. The friction force between species i and j acting on species i then writes $(RT/D_{ij})x_j(\boldsymbol{u_i} - \boldsymbol{u_j})$. Here, $\boldsymbol{u_i}$, respectively $\boldsymbol{u_j}$, denote the molar velocity of species i, respectively j, and D_{ij} is the Maxwell-Stefan diffusivity (or binary diffusion coefficient) between the two components. The constant RT/D_{ij} may then be seen as a drag coefficient. Altogether, this gives the force balance for species i

$$-\frac{1}{c_i}\frac{\mathrm{d}c_i}{\mathrm{d}X} = \sum_{j\neq i}\frac{1}{D_{ij}}x_j(\boldsymbol{u_i} - \boldsymbol{u_j}).$$

If we multiply both sides of the previous equation by x_i, and use $\boldsymbol{N_i} = c_i\boldsymbol{u_i}$, we obtain

$$-\frac{\mathrm{d}x_i}{\mathrm{d}X} = \frac{1}{c_{\mathrm{tot}}}\sum_{j\neq i}\frac{x_j\boldsymbol{N_i} - x_i\boldsymbol{N_j}}{D_{ij}}. \tag{2}$$

Eventually, the reader is invited to check [14] for a better understanding of the physics in this kind of situation.

1.2. **Flux models**

The classical Fick law, which is mostly used for binary mixtures, writes, for any i,

$$\boldsymbol{N_i} = -c_{\mathrm{tot}}F_i\nabla_X x_i, \tag{3}$$

where F_i is the so-called effective diffusion coefficient of species i in the mixture. Since Fick's law only holds for binary mixtures, it means that, for a given species, one only considers the interaction of this species with the whole mixture, and not with each species of the mixture. When F_i is constant, i.e. when the mixture keeps the same conditions of temperature and pressure, and the components do not change a lot, the mole fraction x_i satisfies a linear heat equation, and is not related to the other mole fractions: the system is linear and fully uncoupled.

In the multidimensional version of (2), the Maxwell-Stefan law writes, for any i,

$$-\nabla_X x_i = \frac{1}{c_{\mathrm{tot}}}\sum_{j\neq i}\frac{x_j\boldsymbol{N_i} - x_i\boldsymbol{N_j}}{D_{ij}}. \tag{4}$$

As already stated in 1.1, the coefficients D_{ij}, $i \neq j$, in (4), are the binary diffusion coefficients between species i and j, and happen to satisfy the symmetry property $D_{ij} = D_{ji}$.

We must emphasize that there is a linear dependence between the Maxwell-Stefan laws (4) of all the species. Indeed, it is straightforward that summing (4) over i gives

$$\sum_{i=1}^{M}\nabla_X x_i = \frac{1}{c_{\mathrm{tot}}}\left(\sum_i\sum_{j\neq i}\frac{x_j\boldsymbol{N_i}}{D_{ij}} - \sum_j\sum_{i\neq j}\frac{x_i\boldsymbol{N_j}}{D_{ij}}\right) = 0, \tag{5}$$

because of the symmetry property of the binary diffusion coefficients. Due to this dependence, we must add another equation to our system. This equation must take into account the fact that the behaviour of the mixture is purely diffusive, since we neglect the convection. That implies that there is no global pressure gradient in the

domain, which means that, at each point, the total sum of the fluxes is zero, i.e.

$$\sum_{i=1}^{M} \boldsymbol{N_i} = 0. \tag{6}$$

Because of (1), we can then write that

$$\partial_t \left(\sum_{i=1}^{M} x_i \right) = 0,$$

which corresponds to the total mass conservation:

$$\sum_{i=1}^{M} x_i = 1. \tag{7}$$

Thanks to (7), equation (6) is consistent with (5), and does not linearly depend on (4).

When one chooses the Maxwell-Stefan model, the PDEs satisfied by the mole fractions are not uncoupled and linear anymore, as it was for Fick's law. Because of (4), each flux is strongly related to the others and to all the mole fractions.

Up to our knowledge, there are surprisingly few mathematical studies on this model: numerical analysis [8–10], mathematical analysis [1].

Maxwell-Stefan's law happens to be more relevant in numerous situations, which mainly rise in chemical engineering, see [14]. We first point out its behaviour in the Duncan and Toor experiment, and then investigate its relevance in the framework of the lower airways, as in [2–4, 18]. We find out that the presence of the heliox mixture implies that Fick's law does not hold anymore.

2. Duncan and Toor's experiment

In this section, we study the situation of the Duncan and Toor experiment [6], which provides a simple example of a ternary gas mixture in which the classical Fick law does not hold. Let us first describe the setting of this experiment. We consider two bulbs linked by a capillary tube, see Figure 1. The dimensions of the device, which are recalled below, are given in detail in [6, 17].

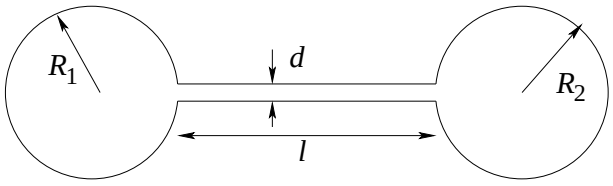

Figure 1. Setting of the Duncan and Toor experiment

The left bulb (bulb 1) has a volume of 77.99 cm^3, and the right one (bulb 2) 78.63 cm^3, which gives numerical values for both bulb radii $R_1 = 26.49$ mm and $R_2 = 26.58$ mm. The length of the capillary tube joining the bulbs is $l = 85.9$ mm and its diameter is $d = 2.08$ mm.

Duncan and Toor study an ideal gas mixture composed of hydrogen, nitrogen and carbon dioxide inside the device. The initial values of the mole fractions of hydrogen (x_1), nitrogen (x_2) and carbon dioxide (x_3) are given by

$$\begin{array}{lll} \text{Bulb 1:} & x_1^{\text{in}} = 0.000, & x_2^{\text{in}} = 0.501, \quad x_3^{\text{in}} = 0.499, \\ \text{Bulb 2:} & x_1^{\text{in}} = 0.501, & x_2^{\text{in}} = 0.499, \quad x_3^{\text{in}} = 0.000. \end{array} \tag{8}$$

For this mixture, the binary diffusion coefficients are the following:

$$D_{12} = 83.3 \text{ mm}^2\,\text{s}^{-1}, \qquad D_{13} = 68.0 \text{ mm}^2\,\text{s}^{-1}, \qquad D_{23} = 16.8 \text{ mm}^2\,\text{s}^{-1}. \tag{9}$$

After opening the stopcock separating the two bulbs, the diffusion of the three species is allowed to happen. Asymptotically in time, the mole fractions reach an equilibrium, i.e. in that case, $x_1^{\text{eq}} = 0.250$, $x_2^{\text{eq}} = 0.500$ and $x_3^{\text{eq}} = 0.250$ everywhere in the device. Note that species 2, i.e. nitrogen, is initially very close to the equilibrium.

We want to compare the behaviour given by our two flux laws defined in Subsection 1.2, for each component. The effective diffusion coefficients can be computed thanks to the Wilke formula, see [20]. For any species i, we have

$$F_i = (1 - x_i^{\text{eq}}) \Bigg/ \left(\sum_{j \neq i} \frac{x_j^{\text{eq}}}{D_{ij}} \right), \tag{10}$$

which ensures, using (9),

$$F_1 = 77.5 \text{ mm}^2\,\text{s}^{-1}, \qquad F_2 = 28.0 \text{ mm}^2\,\text{s}^{-1}, \qquad F_3 = 22.4 \text{ mm}^2\,\text{s}^{-1}. \tag{11}$$

Note that (10) is often used to compute the effective diffusion coefficients, even though it should be limited to the situation when species i is the only one which diffuses, the other components of the mixture being almost stagnant, i.e. $\boldsymbol{N_j} \simeq 0$ for any $j \neq i$. This means that the values of the effective diffusion coefficients given by the Wilke formula are realistic and close to the real ones.

We want to numerically repeat the Duncan and Toor experiment, using the two-dimensional version of the Freefem++ software [12]. It is possible because the device is axisymmetric. We can limit ourselves to consider the upper part of a cutaway view of the device. The mole fractions and the fluxes do not depend on the angle variable, and the angular component of the flux vectors are nil.

With Maxwell-Stefan's laws, we solve the system given by the relation on the fluxes (6)–(7), the second being a consequence of the first, and (1) and (4) for two of the three involved species, with initial data (8) and binary diffusion coefficients given by (9). Using Fick's laws, we solve the system given by (1) and (3) for any i, with initial data (8) and effective diffusion coefficients given by (11). Because of the axisymmetry, we were able to solve two-dimensional problems with cylindrical coordinates to faithfully simulate the three-dimensional situation.

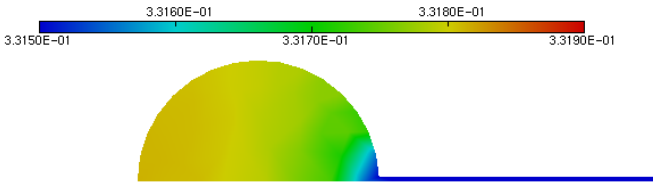

FIGURE 2. Mole fractions x_3 in the left bulb for a Maxwell-Stefan computation ($t = 10$ h)

We first check that, in both Fick and Maxwell-Stefan computations, the values of the mole fractions only depend a little on the location in each bulb. Figure 2 shows, for instance in the Maxwell-Stefan case, that x_3 is almost uniform in the left bulb after ten hours of the experiment, very close to 0.3317. That means that we can equally consider the value of the mole fractions at (almost) every point inside each bulb.

We stick to the situation of the left bulb. On the right side, the situation is of course symmetric because the system is closed. The behaviours of x_1 and x_3 obtained by Fick and Maxwell-Stefan computations are very

similar, as one can see on Figure 3. Nevertheless, we can note that there are some significant variations on the values of x_3. These variations can be explained by the nitrogen behaviour.

As we already stated, nitrogen has almost its equilibrium values in both bulbs, close to 0.5. If the Fick computation brings the awaited behaviour, i.e. $x_2 \simeq$ constant, the Maxwell-Stefan one leads to an *a priori* curious behaviour. One can check the plots on Figure 4.

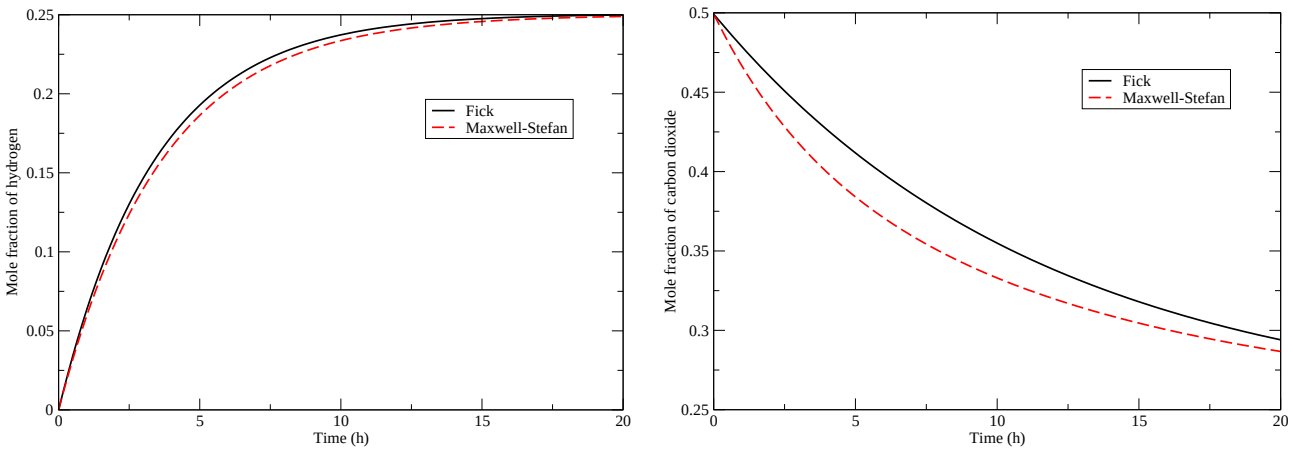

FIGURE 3. Comparison of the mole fractions (a) x_1 and (b) x_3

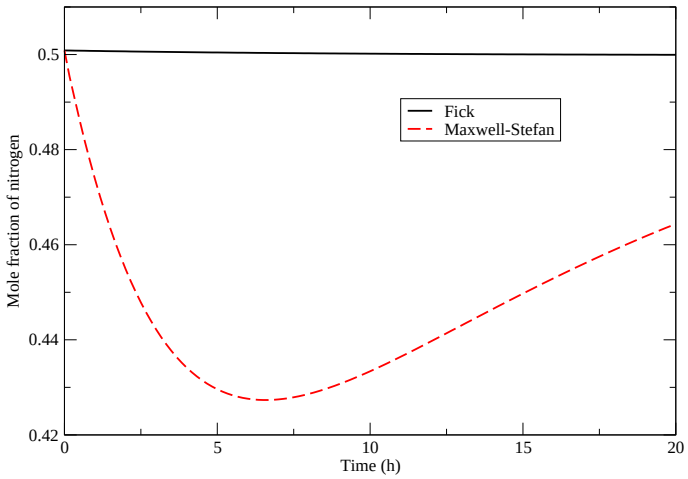

FIGURE 4. Comparison of the mole fractions x_2

In the original experiment by Duncan and Toor [6], they show that x_2 behaves as predicted by the Maxwell-Stefan law. The Fick law is not relevant anymore in this ternary mixture. We can here confirm that fact by observing that the total mass conservation $x_1 + x_2 + x_3 = 1$ for the Fickian mole fractions is not satisfied (the difference goes up 11 % of the value of the sum), as it is shown on Figure 5.

Note that we used the Wilke formula (10) to compute the binary diffusion coefficients. We already emphasized that this use of (10) can be discussed. Nevertheless, we believe that, in this situation, it is not the only reason

why mass is not numerically conserved. Indeed, we can see on Figure 5 that the plot is very similar to the one of $-x_2$, where x_2 is plotted on Figure 4. In particular, they share the same monotonicity at each time. We think that the variations of the Fickian plot of $x_1 + x_2 + x_3 - 1$ is mainly due to the fact that Fick's law cannot generate the behaviour of species 2, which is almost at the equilibrium. Maxwell-Stefan's law accounts for the nitrogen concentration variation, whereas the Fick model gives a constant concentration of this species.

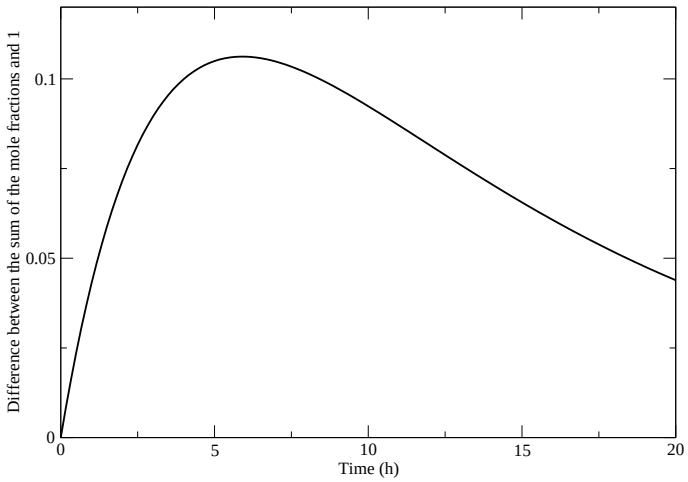

FIGURE 5. Plot of Fick-computed $x_1 + x_2 + x_3 - 1$

The physical behaviour of the three species involved in Duncan and Toor's experiment is explained thanks to the different friction properties of the diffusion pairs. The high concentration gradients of carbon dioxide and hydrogen generate strong fluxes for these species. Due to the larger friction force between carbon dioxide and nitrogen (with respect to the pair hydrogen-nitrogen), carbon dioxide drags nitrogen from the left bulb into the right one, even though its concentration gradient is almost nil. This effect is called the *uphill diffusion*. This leads to a concentration gradient for nitrogen from the less concentrated bulb to the more concentrated one. Together with the decreasing fluxes of species 1 and 2, the mixture eventually reaches a point, called *diffusion barrier*, where this concentration gradient cancels out with the uphill diffusion effect. Beyond this point, the concentration gradient has a stronger effect than the friction forces and hence, the diffusion direction changes. The mixture comes back to the equilibrium, as it would happen for a binary mixture where Fick's law holds. Therefore, the error made by Fick's model is maximal when the uphill diffusion is maximal, and decreases with this phenomenon, and we recover our previous explanation about Figure 5.

3. Oxygen diffusion in the lower airways

3.1. **Medical motivation and chemical setting**

In the following subsections, we study various experimental settings and discuss the behaviours of our two models in the lower airways. If, in 3.4, we only deal with the air (humidified and alveolar), Subsections 3.3 and 3.5 involve a specific mixture of helium and oxygen: heliox.

The interest of such a mixture can be explained in the following way. Let us consider a patient who suffers from a chronic obstructive bronchopneumopathy (COBP), such as asthma. Bronchoconstriction, inflammatory rearrangements of the bronchial mucosa, and mucus hypersecretion imply an increasing resistance of the upper airways to the airflow. This induces an additional respiratory effort for the patient to keep the inspiratory and expiratory rates constant. The effort then results in more fatigue of the lung muscles, e.g. the diaphragm.

To make it simple, the convection of the breathed fresh air towards the acini is more and more difficult, and the patient may eventually need some respiratory support to allow the oxygen to be transported through the proximal bronchial tree and then diffused in the distal one. It consists, for example, in the following procedure. A mixture of oxygen and helium, the so-called heliox, is inhaled by the patient to make the gaseous flow easier. Heliox is composed of about 20% of oxygen, and the rest of helium. Helium is a biologically inactive gaseous species which does not directly act on the inflammation or the bronchocontraction themselves. Since it has no interaction with the airways, and because it lowers the density of the gaseous mixture, it can drive more easily the oxygen towards the acini.

Species	Humidified air	Alveolar air	Humidified heliox	Alveolar heliox
Nitrogen (1)	0.7409	0.7490	0.0000	0.0000
Oxygen (2)	0.1967	0.1360	0.1970	0.1360
Carbon dioxide (3)	0.0004	0.0530	0.0000	0.0530
Water (4)	0.0620	0.0620	0.0620	0.0620
Helium (5)	0.0000	0.0000	0.7410	0.7490

TABLE 1. Composition (mole fractions) of humidified and alveolar air and heliox

Before we compare Fick's and Maxwell-Stefan's models in the lung in Subsections 3.4 and 3.5, we try to numerically reproduce in Subsection 3.3 the experiment described in [18], in which the authors let patients alternatively inhale heliox and fresh air to improve their respiratory situation. Let us recall that the air itself is a gaseous mixture which we keep on assuming to be ideal. It is composed of several species: nitrogen, oxygen, carbon dioxide, water and other species whose concentrations are neglected. The first four species are respectively numbered from 1 to 4. We can find in [11] the various compositions of the air, depending on the lung region where it is located. In this work, we only use two kinds of air: the humidified and alveolar airs, for which the compositions are detailed in Table 1. The humidified air corresponds to the air transported in the upper airways, and we assume that its composition does not change a lot in the proximal tree. The alveolar air is the air coming from the alveoli after the gas exchange with the blood, containing about 5 % of carbon dioxide. Helium is then the fifth species. The composition of the heliox binary mixture varies with respect to the patient situation. In this work, we pick up the values proposed in [18] (0.79 for helium, 0.21 for oxygen) and modify them accordingly for both humidified and alveolar situations. In what follows, we shall refer to each state defined in Table 1 by their names, implying that we impose the corresponding values to each mole fraction.

For the Maxwell-Stefan model, we also need the binary diffusion coefficients for the involved species. Their values are given in Table 2. We once more emphasize that $D_{ij} = D_{ji}$ for any $i \neq j$.

Species	O_2 $(j=2)$	CO_2 $(j=3)$	H_2O $(j=4)$	He $(j=5)$
N_2 $(i=1)$	21.87	16.63	23.15	74.07
O_2 $(i=2)$		16.40	22.85	79.07
CO_2 $(i=3)$			16.02	63.45
H_2O $(i=4)$				90.59

TABLE 2. Binary diffusion coefficients D_{ij} (in $\mathrm{mm}^2\,\mathrm{s}^{-1}$) from [7]

We note that the binary diffusion coefficients involving helium are 3 to 4 times bigger than the other ones, which are all of the same order of magnitude. That implies that the Maxwell-Stefan diffusion process with helium in the mixture will be different. When needed, the effective diffusion coefficients, used for the Fick model, will be given from a reference or estimated thanks to the Wilke formula (10).

3.2. **Computational domain**

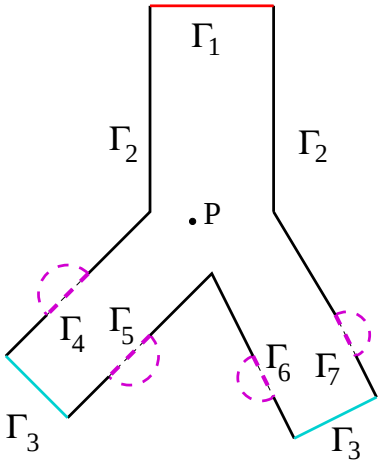

FIGURE 6. Computational domain: two-dimensional branch with alveoli

We are interested in this paper in the lower part of the lung, where the main phenomenon is the diffusion. As already stated, a popular lung model [19] consists in considering a dyadic tree structure with 23 generations. The lower airways approximately correspond to the 15th generation and further. The convection is the main phenomenon happening in the upper airways, and the diffusion is the major one in the lower part. The convection effect decreases with respect to the increasing number of generations. We focus on a computational domain which has the geometry of a two-branch structure, as a subpart of the dyadic tree, as seen on Figure 6. We choose the typical sizes of the 17th generation, i.e. 1.41 mm for the length of the main branch, 0.54 mm for its diameter, whereas the two smaller parts of the branch have a length of 1.17 mm, and a diameter of 0.50 mm.

As a first approximation, we study a two-dimensional setting. This implies that the values of the time scales we shall obtain are not relevant, since the real amount of diffusing matter cannot be conserved in two-dimensional simulations. However, according to comparisons we performed in the Duncan and Toor case, even if the values are not the right ones, the relative order of each phenomenon respectively (i.e. the time evolution of the system) is relevant. This means that the real three-dimensional diffusion time scales are (significantly) larger than the ones we get in the two-dimensional computations, but the distribution of the phenomena in time is conserved.

The boundary of this domain is divided into several parts: the wall Γ_2, the "entrance" Γ_1, the "exits" Γ_3 and the alveoli Γ_k, $4 \leq k \leq 7$. We consider a geometry with four alveoli boundaries. This number 4 is not really significant here, and we could have chosen other values. Note that the alveoli themselves are not geometrically included in the domain, and we do not model the gas exchange. The numerical results presented below are the mole fractions of the involved species at some point P of the domain, near the junction of the branch, as in Figure 6.

In the following subsections, the Maxwell-Stefan solving uses equations (1) and (4) for species 2 to 4 (or 5, when helium is involved), and equations (6)–(7) for species 1. When comparing with Fick's law, we solve equations (1) and (3) for all the involved species. The initial data as well as the boundary conditions are given in each subsection. Note that, unlike in Section 2, we need boundary conditions, because the system we study is not closed anymore. There are no condition on the fluxes, and we choose mixed boundary conditions on the mole fractions, i.e. we impose a homogeneous Neumann boundary condition on Γ_2 (nothing goes in or out through the walls) and fitted Dirichlet boundary conditions on the remaining boundary. For instance, in the

inhaling case, we impose the values of the mole fractions corresponding to humidified air or heliox on Γ_1, and to alveolar air or heliox on Γ_k, $k \geq 3$.

We could have taken Dirichlet boundary conditions for the fluxes on the alveoli, but we chose to have boundary conditions on the mole fractions everywhere. Imposing the values of the mole fractions on Γ_k, $k \neq 2$, means that we consider the rest of the respiratory system and the alveoli to be long-time suppliers of the gaseous mixture imposed on the corresponding boundary.

3.3. **Heliox and air alternate inhaling**

The first numerical experiment aims to repeat the *in vivo* experiment described in [18] (see also [2]). Thiriet *et al.* consider a set of patients suffering from COBP. They make them inhale heliox during twenty minutes, and then fresh air for fifteen to twenty minutes, then again heliox and fresh air for the same periods. They eventually observe an improvement of the respiratory situation of the patients.

We here use the Maxwell-Stefan model, because we have reliably the associated binary diffusion coefficients at our disposal. At the beginning of our computation, the domain is filled with alveolar air. Since the rest of the airways is not integrated in our computational domain, we impose physically relevant values of the mole fractions on the boundaries. These boundary conditions correspond to having some large volume (with respect to the volume of the branch) persistently supplying each component of the mixture with its corresponding mole fraction. At the entrance Γ_1, we have incoming humidified air, and, at the exits Γ_3 and the alveoli, we have alveolar air. Then, after reaching some equilibrium between the humidified and alveolar airs at each point, the experiment begins, and the boundary condition on Γ_1 is set to humidified heliox: the heliox binary mixture gains water during the convection in the upper airways. The other boundary conditions are unchanged for the moment. When the oxygen mole fraction reaches 90 % of its equilibrium value, the boundary conditions are again modified. We set humidified air at Γ_1, and alveolar heliox at Γ_3 and the alveoli. Of course, there is a jump of the boundary conditions. In fact, we should consider time-continuous data, but we eventually get the same kind of behaviours. Anyway, the boundary conditions changes iteratively, and this process (inhaling heliox, then fresh air) happens twice. We obtain Figures 7–8.

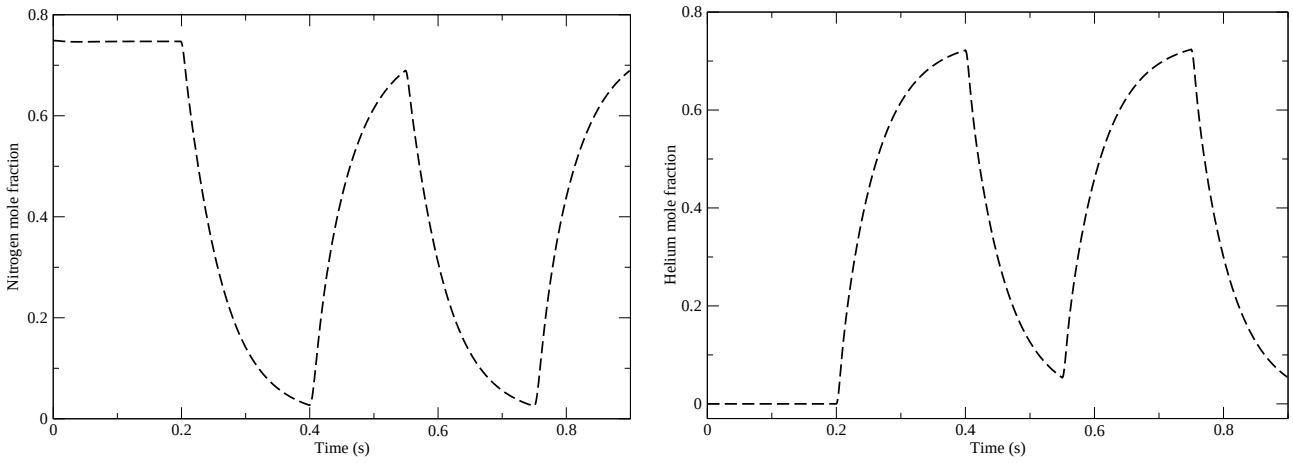

FIGURE 7. Alternate experiment: behaviour of the mole fractions of (a) N_2 and (b) He

Let us give some details about the sequence of events. The experiment starts at 0.2 s (at the equilibrium), the heliox inhaling happens between 0.2 and 0.4 s, humidified air boundary conditions are imposed between

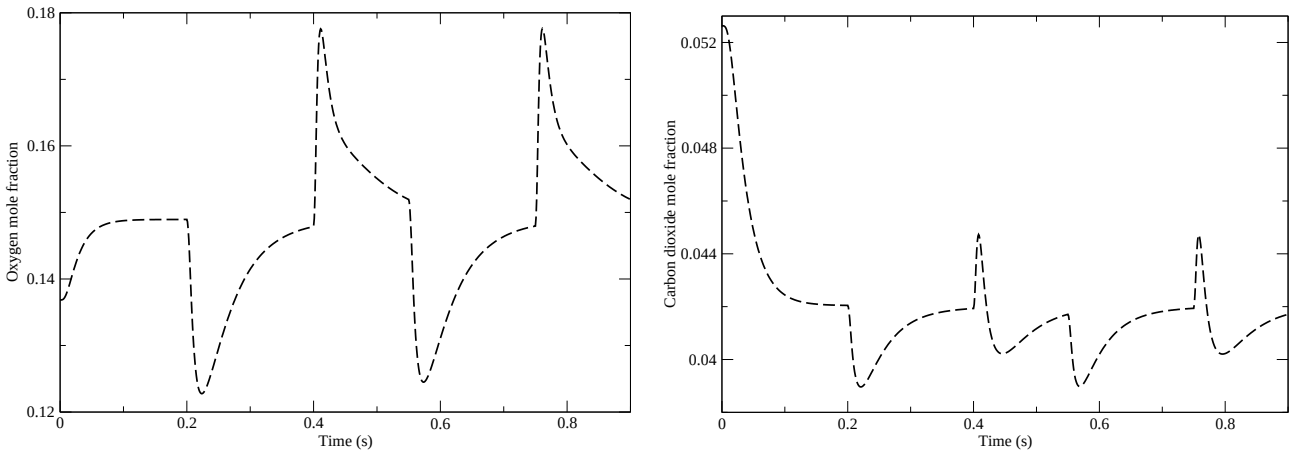

FIGURE 8. Alternate experiment: behaviour of the mole fractions of (a) O_2 and (b) CO_2

0.4 and 0.55 s, and the whole process repeats between 0.55 and 0.9 s. We can see on Figure 7 that the heliox inhaling stage allows to fill the lower airways with (humidified) heliox, and almost all of the nitrogen is replaced by helium. On Figure 8(b), we can see that the outgoing carbon dioxide is favoured. On the contrary, at the same stage, we see, on Figure 8(a), an inconvenient peak of oxygen mole fraction. At first sight, this would lead us not to use heliox anymore. Nevertheless, let us recall that heliox is more easily transported than the air itself, in the inflamed upper airways. Hence, this bad variation of x_2 seems to be widely balanced by the time gain and the non-aggressive properties of helium during the convection. After fifteen minutes, we can hope that the inflammation is a little bit calmed down. The patient then inhales fresh air, which also becomes humidified when it goes down to the 17th generation. Then, this time, we obtain on Figure 8(a) a much better behaviour of the oxygen mole fraction, with a significant increasing. Note that we eventually obtain the same amount of diffused oxygen as if we kept incoming humidified air, but this behaviour is still beneficial from a medical point of view.

As we already pointed out, the time scales are not good in the two-dimensional setting, and we also miss many properties of the transport and diffusion of the air in the lung. The branch we consider is very small with respect to the actual size of the airways. The twenty minutes Thiriet *et al.* speak about in [18] concern the full respiratory system and not the small part we here study. Nevertheless, we were able to recover the main behaviour of heliox and air in the lung.

3.4. **Diffusion models for the air**

This subsection and the next one are dedicated to the comparison between Fick's and Maxwell-Stefan's diffusion laws. In this first test, the initial datum in the domain is the alveolar air. Humidified air goes in through Γ_1, and the exits and alveoli have an alveolar air boundary condition. For the Fick computation, we use the effective diffusion coefficients given in [7] as binary coefficients for a species with regard to the air, i.e. (in $\mathrm{mm}^2\,\mathrm{s}^{-1}$)

$$F_1 = 21.71, \qquad F_2 = 21.95, \qquad F_3 = 16.60, \qquad F_4 = 23.13. \tag{12}$$

We can see in (12) that the effective diffusion coefficients are of the same order. In fact, they also share the same order of magnitude as the binary diffusion coefficients of each pair of species, and in this case, we can compare the Fick and the Maxwell-Stefan equations (3) and (4). For the sake of simplicity, let us a consider a

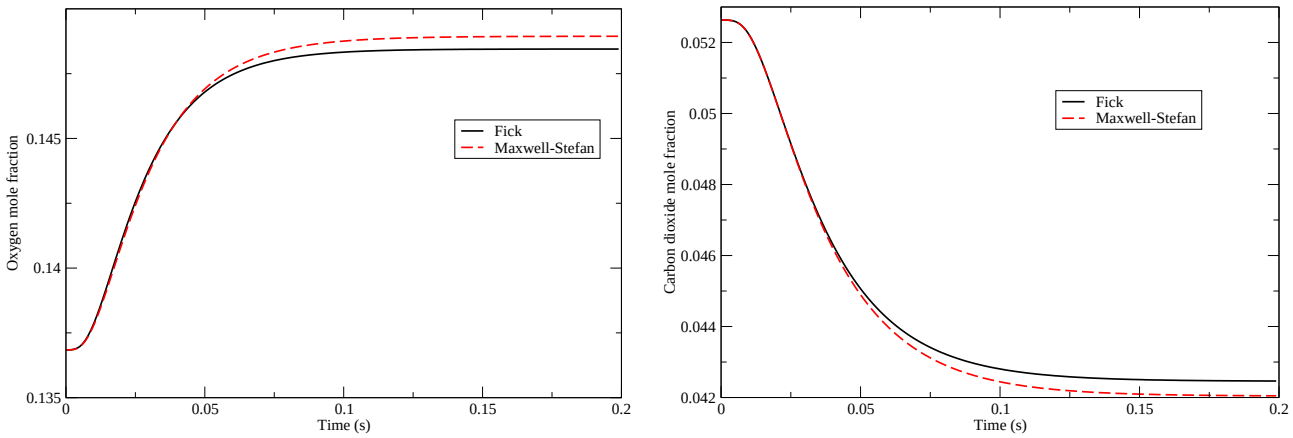

FIGURE 9. Air alone: comparison of the mole fractions of (a) O_2 and (b) CO_2

constant F such that $D_{ij} \simeq F$ for any species $i \neq j$. We can write, from (4),

$$-\nabla_X x_i \simeq \frac{1}{c_{\text{tot}} F} \sum_{j \neq i} (x_j \boldsymbol{N_i} - x_i \boldsymbol{N_j}) = \frac{1}{c_{\text{tot}} F} (\boldsymbol{N_i}(1 - x_i) + x_i \boldsymbol{N_i}),$$

because of (6)–(7). We eventually recover Fick's law (3) with $F_i \simeq F$ for any i. Hence the behaviours of the mole fractions following each model are very similar, see Figure 9. Thanks to Table 2, we know that the binary diffusion coefficients involving helium are not of the same order of magnitude as the other ones. The previous considerations imply that Fick's and Maxwell-Stefan's laws do not behave in the same way when there is helium in the mixture (see Subsection 3.5).

On Figure 9, we can note that there are two different equilibrium values for the mole fractions corresponding to each model. This seems to be only an effect of the choice of the effective diffusion coefficients (12). These ones may be effective coefficients in a dry air. Eventually, we do not show any plot for nitrogen, because both models give almost constant behaviours.

3.5. **Diffusion models for the air/heliox mixture**

In the second test, the initial datum in the domain is the alveolar heliox. The boundary conditions are the following ones: humidified air on Γ_1, alveolar heliox on the exits and the alveoli. This time, since helium is involved, we have to use Wilke's formula (10) to compute the effective diffusion coefficients. The problem is that the equilibrium values are not uniform anymore in space, as in Section 2, they depend on the location of the measurement point P. Nevertheless, asymptotically in time, since there is eventually no helium going in the branch, we chose the alveolar air as the asymptotic state, which does not depend on the location. Note that these asymptotic values are not compatible with the alveolar heliox boundary conditions, but they correspond to the fact that eventually, all of the helium leaves the lung. We then obtain the following values of the effective diffusion coefficients (in $\text{mm}^2\,\text{s}^{-1}$):

$$F_1 = 20.78, \qquad F_2 = 21.50, \qquad F_3 = 16.55, \qquad F_4 = 22.54, \qquad F_5 = 74.90.$$

In Figure 10, one can check that both oxygen and carbon dioxide have very different and numerically significant behaviours. The uphill diffusion occurs for both species, and it is clear that Fick's law does not hold in this situation. Of course, as we can see on Figure 11, the two involved carriers, nitrogen and helium, give very

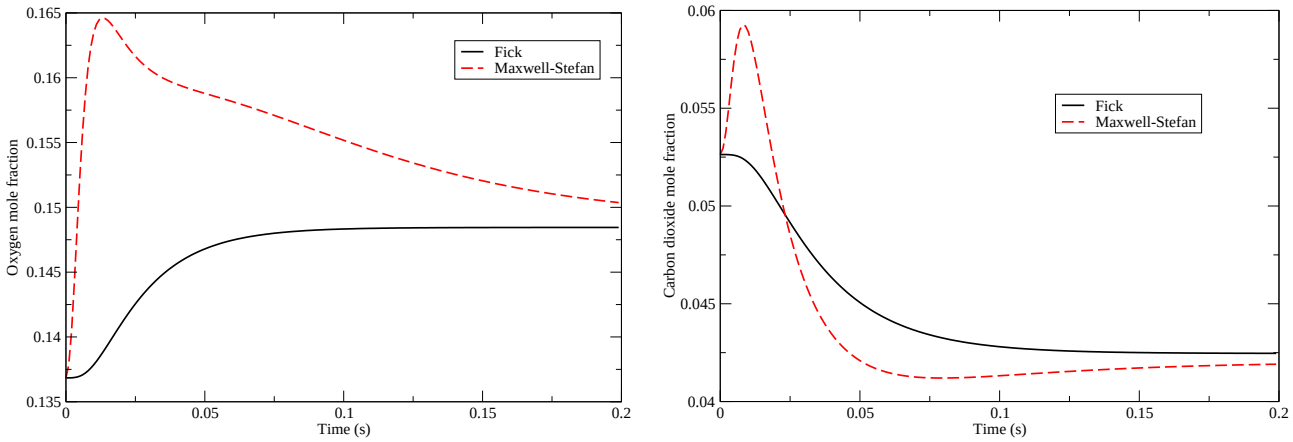

FIGURE 10. Air-heliox: comparison of the mole fractions of (a) O_2 and (b) CO_2

similar behaviours using both models. The helium mole fraction plots are even almost exactly superimposed, probably because of the higher values of the diffusion coefficients.

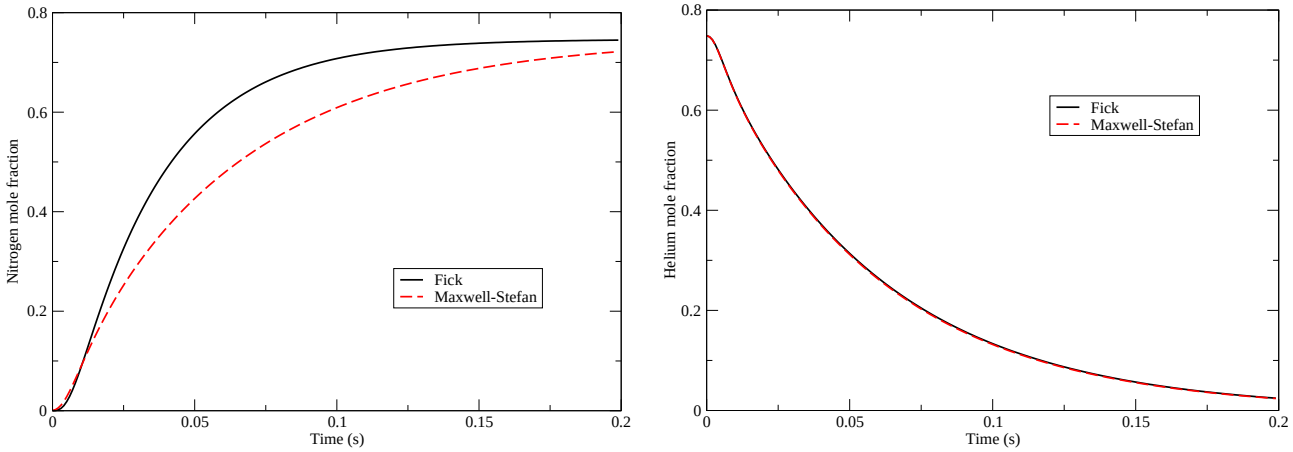

FIGURE 11. Air-heliox: comparison of the mole fractions of (a) N_2 and (b) He

PROSPECTS

As the results obtained in 3.4 show it, the air diffusion can be modelled using Fick's law in most situations. We proved that it is mainly due to the fact that the binary diffusion coefficients of all species involved in the air mixture approximately have the same order of magnitude, around 20 $mm^2\,s^{-1}$. When we add a species whose binary diffusion coefficients are not of the same order, such as helium, Fick's law must be replaced by Maxwell-Stefan's law. The heliox mixture, whose composition can vary accordingly to the patient's needs, happens to be a really good solution in case of COBP. Moreover, heliox can also be used as an aerosol carrier, instead of the air. If we intend to study an aerosol behaviour in the lower airways, we may need to couple the aerosol equations with either Fick's or Maxwell-Stefan's model.

In parallel, we must also try to improve the boundary conditions on our domain. We assumed that the open boundaries, where we impose Dirichlet boundary conditions, can be seen as some kind of infinite bulbs, as in the Duncan and Toor experiment, providing an infinite amount of the present species to our domain. For our time scales, it does not seem so wrong, but eventually, for a permanent breathing process, it cannot be relevant. In particular, the boundary condition at the entrance should be driven by what comes from the upper airways, so it is clearly at least time-dependent and continuous.

Eventually, of course, to obtain more realistic time scales, we should work in a three-dimensional setting. And we bump again into the fact that there is no possible medical imaging of the lower airways. That means that we may need to work in an adapted geometry, such as Kitaoka *et al.*'s acinus.

Acknowledgments

The authors want to thank Anne Devys for making the working atmosphere productive and lovely, and with whom the discussions have always been fruitful. They are also grateful to Francesco Salvarani and Marc Thiriet for the precious pieces of information they provided to support their Cemracs project.

References

[1] L. Boudin, B. Grec, and F. Salvarani. A mathematical and numerical analysis of the Maxwell-Stefan diffusion equations, 2010. submitted.
[2] H.K. Chang. Multicomponent diffusion in the lung. *Fed. Proc.*, 39(10):2759–2764, 1980.
[3] H.K. Chang and L.E. Farhi. Ternary diffusion and effective diffusion coefficients in alveolar spaces. *Respir. Physiol.*, 40(2):269–279, 1980.
[4] H.K. Chang, R.C. Tai, and L.E. Farhi. Some implications of ternary diffusion in the lung. *Respir. Physiol.*, 23(1):109–120, 1975.
[5] J. Crank. *The mathematics in diffusion*. Clarendon Press, Oxford, 1975.
[6] J.B. Duncan and H.L. Toor. An experimental study of three component gas diffusion. *AIChE Journal*, 8(1):38–41, 1962.
[7] L.A. Engel and M. Paiva, editors. *Gas mixing and distribution in the lung*, volume 25 of *Lung biology in health and disease*. Marcel Dekker, Inc., 1985.
[8] A. Ern and V. Giovangigli. Projected iterative algorithms with application to multicomponent transport. *Linear Algebra Appl.*, 250:289–315, 1997.
[9] V. Giovangigli. Convergent iterative methods for multicomponent diffusion. *Impact Comput. Sci. Engrg.*, 3(3):244–276, 1991.
[10] V. Giovangigli. *Multicomponent flow modeling*. Modeling and Simulation in Science, Engineering and Technology. Birkhäuser Boston Inc., Boston, MA, 1999.
[11] A.C. Guyton and J.E. Hall. *Textbook of Medical Physiology*. Elsevier Saunders, 11th edition, 2006.
[12] F. Hecht, A. Le Hyaric, K. Ohtsuka, and O. Pironneau. Freefem++, finite elements software, `http://www.freefem.org/ff++/`.
[13] H. Kitaoka, S. Tamura, and R. Takaki. A three-dimensional model of the human pulmonary acinus. *J. Appl. Physiol.*, 88(6):2260–2268, 2000.
[14] R. Krishna and J.A. Wesselingh. The Maxwell-Stefan approach to mass transfer. *Chem. Eng. Sci.*, 52(6):861–911, 1997.
[15] B. Mauroy. *Hydrodynamics in the lungs, relations between flows and geometries*. PhD thesis, ENS Cachan, 2004.
[16] B. Sapoval, M. Filoche, and E.R. Weibel. Smaller is better – but not too small: A physical scale for the design of the mammalian pulmonary acinus. *Proc. Natl. Acad. Sci. U.S.A.*, 99(16):10411–10416, 2002.
[17] R. Taylor and R. Krishna. *Multicomponent mass transfer*. John Wiley & Sons, Inc., 1993.
[18] M. Thiriet, D. Douguet, J.-C. Bonnet, C. Canonne, and C. Hatzfeld. The effect on gas mixing of a He-O_2 mixture in chronic obstructive lung diseases. *Bull. Eur. Physiopathol. Respir.*, 15(5):1053–1068, 1979. In French.
[19] E.R. Weibel. *The pathway for oxygen: structure and function in the mammalian respiratory system*. Harvard University Press, 1984.
[20] C.R. Wilke. Diffusional properties of multicomponent gases. *Chem. Engng Prog.*, 46:95–104.